International Journal of Engineering Science 202 (2024) 104103

Contents lists available at ScienceDirect

International Journal of Engineering Science

journal homepage: www.elsevier.com/locate/ijengsci

A neat flux-based weak formulation for thermal problems which develops Biot's variational principle

Ali Haydar [a], Laura Galuppi [a], Gianni Royer-Carfagni [a,b,*]

[a] Department of Engineering for Industrial Systems and Technologies, University of Parma, Parco Area delle Scienze 181/A, I-43124 Parma, Italy

[b] Construction Technologies Institute - Italian National Research Council (ITC-CNR), Via Lombardia 49, I-20098 San Giuliano Milanese, Milano, Italy

ARTICLE INFO

Keywords:
Thermal analysis
Variational approach
Transient heat transfer
Computation
Composite material

ABSTRACT

We propose a weak form of the transient heat equations for solid bodies, as a time-dependent spatial variation of the heat displacement vector field, whose time derivative is the heat flux. This develops the variational principle originally proposed by Biot, inasmuch Fourier's law is embedded as a holonomic constraint, while energy conservation results from the variation (the vice-versa from Biot). This is a neat formulation because only the heat displacement appears in the variational equations, whereas Biot's form also involved the unknown temperature field: Fourier's law is used only *a posteriori* to recover the temperature. Since the heat displacement is generally more regular than the temperature field, it represents a natural variable in problems with material inhomogeneities, uneven radiation, thermal shocks. The three-dimensional analytical set-up is presented in comparison with Biot's, for boundary conditions accounting for radiation and convection. A mechanical analogy with the equilibrium of an elastic bar with viscous constraints is suggested for the one-dimensional case. The variational equations are implemented in a finite element code. Numerical experiments on benchmark problems, involving high temperature gradients, confirm the efficiency of the proposed approach in many structural problems.

1. Introduction

No structural designer can avoid addressing issues regarding temperature, thermal stress, and material properties. Thermal strain can produce stress states well beyond the material capacity if the motion is incompatible with the constraints. Uneven temperature distributions may induce an eigenstress state in unconstrained bodies. Composite structures are characterized by the association of materials with different thermal properties, which may provoke stress concentrations, especially at the interfaces and at the edges (Groh & Weaver, 2016; Mittelstedt, Becker, Kappel, & Kharghani, 2022). Portions with very high or very low thermal transmissivity can be artfully incorporated into a structural organism to convey the heat flow into the body to reduce stress state. For problems involving high temperatures, high temperature gradients and cyclical changes of temperature, thermo-physical and mechanical properties of constituent materials may vary as a function of the temperature (Galuppi, Franco, & Bedon, 2023; Noda, 1991).

In many practical problems of civil, mechanical, nuclear, aeronautical and aerospace engineering, the temperature field cannot be represented by smooth functions in space and time. This occurs in the presence of thermal shocks, uneven heat sources, materials

* Corresponding author at: Department of Engineering for Industrial Systems and Technologies, University of Parma, Parco Area delle Scienze 181/A, I-43124 Parma, Italy.
E-mail address: gianni.royer@unipr.it (G. Royer-Carfagni).

https://doi.org/10.1016/j.ijengsci.2024.104103
Received 16 January 2024; Received in revised form 21 May 2024; Accepted 1 June 2024
Available online 20 June 2024

with inhomogeneous thermal properties (Furmański, 1997; Wang, Guo, & Wang, 2023; Wang, Li, & Yang, 2015) (laminates, long and short fiber-reinforced, inclusion-filled, polycrystalline). However, the paradigm in all models is Fourier's law of thermal conduction, which involves the gradient of the temperature field. This may cause problems in the presence of strong irregularities, especially when these occurs in regions of the body not known a priori. The difficulties are evident especially in the numerical discretization. Standard numerical approaches for thermal problems (Carter & Booker, 1989; Zienkiewicz, Taylor, & Zhu, 2005) are formulated in terms of the temperature field only, and based on standard finite element approach in space, relying on the Weighted Residual Method, and on a finite difference approximation of the time-dependence of the relevant field. Simpler methods are often used, consisting in discretizing the governing equation of the problem by means of finite difference techniques, in both space and time (Ismail & Henríquez, 2003; Strobel, Abadie, & Mendes, 2007). In most of these approaches, the condition of energy conservation is only approximately satisfied.

In the 1950's Biot (1955) proposed an ingenious weak form of the heat conduction equation starting from the definition of the *heat displacement* vector field, whose time derivative is the heat flux. Such field enjoys a higher regularity with respect to the temperature field and, therefore, allows to directly consider complex problems. Moreover, the variational form of the equations permits a straightforward finite element implementation in space. Biot further observed (Biot, 1970) that the resulting equations are of the same form as those of Lagrangian mechanics for the slow motion of a dissipative system with negligible inertia forces, defined by the potential energy and the dissipation function. The temperature distribution at the boundary and the heat sources provide thermal driving forces, defined by the method of virtual work as in mechanics (hence, called *thermal forces*). Personally, we find this analogy very enlightening for an intuitive interpretation of heat diffusion phenomena at the qualitative level.

Since Biot referred to his formulation as a variational principle in heat transfer (Biot, 1970), we will continue here to use this name. However, it should be mentioned that it is not a true variational principle because of its reliance on the Rayleigh dissipation function concept. The dissipation function is not defined, but only the supposed variation of the dissipation function is set to the form needed to recover the governing differential equations of the problem. Although this approach has sometimes been reputed of limited fundamental appeal and can lead to other difficulties in the problem solution, especially for highly dissipative systems, we repute it very interesting for most applications of structural engineering, for which the material properties are accurately defined by a few coefficient and not affected by chemical or nuclear transformations.

The original form of Biot's variational principle corresponds to the weak form of Fourier's equation, written in terms of both the temperature and heat displacement fields, where the energy conservation law is a holonomic constraint to be satisfied. We recall that Biot also proposed (Biot, 1967) a complementary principle, where the heat flux is defined in terms of the temperature and the variational principle is expressed in terms of the variation of the temperature field. Other variational principles, bearing some analogy with it, have been developed (Chambers, 1956; Lorenzini, 1970; Rosen, 1953). Here, we propose a new variational formulation of the thermal problem that we may attempt to call "neat" because the variational equations are written in terms of the heat displacement field only. It develops, while preserving, Biot's idea, because it provides the weak form of the energy conservation law, whereas Fourier's equation is "embedded" in the variational form. Specifically, the constraint provided by Fourier's equation, and hence the temperature field, does not explicitly appear in the resulting equations. The constraint shall be used only a posteriori, to calculate the temperature field in the body once the heat displacement field has been obtained.

The variational approach is formulated for three-dimensional bodies under various types of boundary conditions. The one-dimensional version also suggests an intuitive mechanical analogy with the problem in structural mechanics of a linear elastic rod subjected to viscous constraints (dashpots). A numerical FEM implementation is proposed, based on the use of the simplest tri-linear shape functions to approximate the heat displacement field.

This work complements and extends the numerical method developed in Galuppi and Royer-Carfagni (2022), specifically conceived for the one-dimensional thermal analysis of laminated glass window panes, which was based on the original Biot's principle. This evidenced a major draw-back, since it necessitated to discretize both the heat displacement and the temperature fields with high order Hermite shape functions. That approach was further extended (Galuppi & Royer-Carfagni, 2023a, 2023b) to the three dimensional case, with the specific aim of evaluating the uneven temperature fields and heat fluxes in architectural glazing under varying uneven external conditions (temperature and solar radiation), but provided a spurious behavior of the temperature field at the critical points. The numerical approach via the flux-based "neat" variational principle is easier to implement and more accurate.

The article is organized as follows. Section 2 presents the new variational principle, detailing the resulting field equations under various boundary conditions. An analogy with the mechanics of an elastic bar is proposed for the one-dimensional case. In Section 3, the principle is implemented in a finite element framework, and applied to paradigmatic benchmark problems, illustrated in Section 4. The major outcomes from this research and hints for future work are proposed in the Conclusions.

2. Variational approaches for the thermal problem

Let the three-dimensional domain Ω denote the reference configuration of a solid body, with boundary $\partial\Omega$ and outer unit normal $\mathbf{n}$. Introduce the right-handed reference system (x, y, z), and indicate with $\theta(\mathbf{x}, t)$ the temperature at the point $\mathbf{x} = (x, y, z)$ at time t. The body exchanges heat with the external environment via convection and radiation.

2.1. Heat displacement field and differential form of the thermal problem

Following the seminal work by Biot (1970), it is useful to write (as usual $\dot{(\,)}$ indicates time derivative) the local rate of heat flow as $\dot{\mathbf{H}}(\mathbf{x},t)$, where $\mathbf{H}(\mathbf{x},t)$ is the *heat displacement field*. Denoting with λ the thermal conductivity of the material, the thermal problem is governed by classical Fourier's law (Lienhard & Lienhard, 2019), which reads

$$\lambda\ \nabla\theta(\mathbf{x},t)+\dot{\mathbf{H}}(\mathbf{x},t)=\mathbf{0}\,,\ \forall\mathbf{x}\in\Omega\,,\quad\forall t\,. \tag{2.1}$$

Energy conservation provides that, for any sub-body $\mathcal{B}\subset\Omega$ with outer unit normal $\mathbf{n}$,

$$-\int_{\partial\mathcal{B}}\dot{\mathbf{H}}(\mathbf{x},t)\cdot\mathbf{n}\ ds+\int_{\mathcal{B}}q^{\sharp}(\mathbf{x},t)\ dV=\int_{\mathcal{B}}c\,\dot{\theta}(\mathbf{x},t)\ dV\,, \tag{2.2}$$

where c is the material specific heat per unit volume and $q^{\sharp}(\mathbf{x},t)$ is the generated/absorbed heat per unit volume and unit time.

In general, c and λ may vary within the body and be temperature dependent, but for our specific application, they will be supposed constant. Moreover, internal production/dissipation mechanisms may affect the form of $q^{\sharp}(\mathbf{x},t)$, but this is not considered here: $q^{\sharp}(\mathbf{x},t)$ will be treated as a problem datum, associated with heat radiation, and no internal phenomena of dissipation are supposed to be present. This is a strong assumption, but it is verified for most applications of structural engineering.

Integrating (2.2) by parts, since the sub-body $\mathcal{B}\in\Omega$ is arbitrary, the local form of energy conservation can be written as

$$-\nabla\cdot\dot{\mathbf{H}}(\mathbf{x},t)+q^{\sharp}(\mathbf{x},t)=c\ \dot{\theta}(\mathbf{x},t)\,,\ \forall\mathbf{x}\in\Omega\,,\quad\forall t\,. \tag{2.3}$$

A particular case (*steady state* condition) is that in which $q^{\sharp}(\mathbf{x},t)=0$ and $\dot{\theta}(\mathbf{x},t)=0$, which provides $\nabla\cdot\dot{\mathbf{H}}(\mathbf{x},t)=0$. More in general, using (2.1) in (2.3), one obtains the heat diffusion equation (Lienhard & Lienhard, 2019)

$$\Delta\theta(\mathbf{x},t)+q^{\sharp}(\mathbf{x},t)=c\ \dot{\theta}(\mathbf{x},t)\,,\ \forall\mathbf{x}\in\Omega\,,\quad\forall t\,. \tag{2.4}$$

Following again Biot (1970), it is convenient to define the fictitious heat flux $\dot{\mathbf{H}}^{\sharp}(\mathbf{x},t)$, associated with $q^{\sharp}(\mathbf{x},t)$ via

$$\int_{\mathcal{B}}q^{\sharp}(\mathbf{x},t)\ dV=-\int_{\partial\mathcal{B}}\dot{\mathbf{H}}^{\sharp}(\mathbf{x},t)\cdot\mathbf{n}\ ds\quad\Rightarrow\quad\nabla\cdot\dot{\mathbf{H}}^{\sharp}(\mathbf{x},t)=-q^{\sharp}(\mathbf{x},t)\,,\ \forall\mathbf{x}\in\Omega\,,\quad\forall t\,. \tag{2.5}$$

In this formulation we consider (Biot, 1970), as relevant vector fields for the thermal problem, the *heat displacements* $\mathbf{H}(\mathbf{x},t)$ and $\mathbf{H}^{\sharp}(\mathbf{x},t)$, as the time integral of the corresponding heat fluxes, i.e.,

$$\mathbf{H}(\mathbf{x},t)\ :=-\int_0^t\lambda\nabla\theta(\mathbf{x},t)\ dt\,, \tag{2.6a}$$

$$\mathbf{H}^{\sharp}(\mathbf{x},t)\ :=\int_0^t\dot{\mathbf{H}}^{\sharp}(\mathbf{x},t)\ dt\,,\quad\nabla\cdot\mathbf{H}^{\sharp}(\mathbf{x},t)=-\int_0^t q^{\sharp}(\mathbf{x},t)\ dt\,, \tag{2.6b}$$

for which the values at $t=0$ can be assumed null, without loss of generality. It is clear (Biot, 1970), from (2.3) and (2.5), that the heat displacements will be defined up to an additive time-independent solenoidal vector, but this is indeterminacy is inessential in the solution of the thermal problem (Galuppi & Royer-Carfagni, 2022). Then, Eq. (2.2) can be integrated in time, to give

$$-\int_{\mathcal{B}}\nabla\cdot\left[\mathbf{H}(\mathbf{x},t)+\mathbf{H}^{\sharp}(\mathbf{x},t)\right]\ dV=\int_{\mathcal{B}}c\left[\theta(\mathbf{x},t)-\theta_0(\mathbf{x})\right]\ dV\,, \tag{2.7}$$

where $\theta_0(\mathbf{x}):=\theta(\mathbf{x},0)$ is the initial temperature distribution in the body. The local form of the energy balance is therefore

$$-\nabla\cdot\left[\mathbf{H}(\mathbf{x},t)+\mathbf{H}^{\sharp}(\mathbf{x},t)\right]=c\left[\theta(\mathbf{x},t)-\theta_0(\mathbf{x})\right]\,,\ \forall\mathbf{x}\in\Omega\,,\quad\forall t\,. \tag{2.8}$$

As indicated by Biot (1970), the main advantage is that the energy conservation law (2.8) now does not involve any time derivative.

2.2. "Classical" form of the variational principle

The variational principle, here called "classical", was proposed by Biot (1970), but with a different definition of the displacement field, which we prefer not to follow here for the reasons explained in Remark 2.1. Essentially, it provides the weak form of Fourier's equation, whereas the energy conservation law plays the role of a holonomic constraint.

After multiplying (2.1) for the variation of the displacement field $\delta\mathbf{H}$ (whose dependence on $(\mathbf{x},t)$ is not written for brevity), integration over Ω provides

$$\int_{\Omega}\nabla\theta(\mathbf{x},t)\ \cdot\delta\mathbf{H}\ dV+\int_{\Omega}\frac{1}{\lambda}\ \dot{\mathbf{H}}(\mathbf{x},t)\ \cdot\delta\mathbf{H}\ dV=0\,. \tag{2.9}$$

To account for energy conservation, $\delta\mathbf{H}$ should be chosen such to satisfy (2.8). Observe that, since $\mathbf{H}^{\sharp}(\mathbf{x},t)$ and $\theta_0(\mathbf{x})$ are assigned, then $\delta\mathbf{H}^{\sharp}(\mathbf{x},t)=\mathbf{0}$ and $\delta\theta_0(\mathbf{x})=0$; consequently

$$-\nabla\cdot\delta\mathbf{H}(\mathbf{x},t)=c\ \delta\theta(\mathbf{x},t)\,. \tag{2.10}$$

Therefore, integrating (2.9) by part and using (2.10), one obtains

$$\int_\Omega c\ \theta(\mathbf{x},t)\ \delta\theta\ dV + \int_\Omega \frac{1}{\lambda}\ \dot{\mathbf{H}}(\mathbf{x},t)\cdot\delta\mathbf{H}\ dV = -\int_{\partial\Omega}\theta(\mathbf{x},t)\ \delta\mathbf{H}\cdot\mathbf{n}\ ds\,. \tag{2.11}$$

This provides the variational principle, which has to be complemented with Eq. (2.8), which correlates the field variables $\mathbf{H}(\mathbf{x},t)$ and $\theta(\mathbf{x},t)$.

It is straightforward to demonstrate that the first variation of (2.11) with the constraint (2.8) provides Fourier's law. This results from an arbitrary variation $\delta\mathbf{H}$ and the corresponding variation of $\delta\theta$ according to (2.10). However, a major drawback of this approach is that both the fields $\theta(\mathbf{x},t)$ and $\mathbf{H}(\mathbf{x},t)$ enter in the equations, and they are related by the constraint.

Remark 2.1 (*The Original Formulation by Biot*)**.** The formulation originally proposed by M. Biot in the 1950's (Biot, 1957, 1970), relies upon an alternative definition of the heat flux fields. In particular, $q^\sharp(\mathbf{x},t)$ is defined via the vector field $\mathbf{H}^*(\mathbf{x},t)$, opposite to $\mathbf{H}^\sharp(\mathbf{x},t)$ of (2.5), i.e.,

$$\nabla\cdot\mathbf{H}^*(\mathbf{x},t) = \int_0^t q^\sharp(\mathbf{x},t)\ dt\,. \tag{2.12}$$

The counterpart of the energy conservation law (2.8) is now

$$-\nabla\cdot\mathbf{H}^+(\mathbf{x},t) = c\ \left[\theta(\mathbf{x},t)-\theta_0(\mathbf{x})\right]\,,\ \forall\mathbf{x}\in\Omega\,,\quad\forall t\,. \tag{2.13}$$

where the field $\mathbf{H}^+(\mathbf{x},t)$ is a *fictitious* heat displacement, since it is not directly correlated with the heat flux.

Probably, these definitions are consequent to the genesis of the principle. Biot first defined the variational principle in absence of heat source, and then added the contribution of the generated heat. By comparing Eqs. (2.13) and (2.8), it can be verified that $\mathbf{H}^+(\mathbf{x},t)=\mathbf{H}(\mathbf{x},t)+\mathbf{H}^\sharp(\mathbf{x},t)$: there is no difference when $\mathbf{H}^\sharp(\mathbf{x},t)=\mathbf{0}$. In this framework, Fourier's law (2.1) is written as (Biot, 1970)

$$\lambda\ \nabla\theta(\mathbf{x},t)+\dot{\mathbf{H}}^+(\mathbf{x},t)+\dot{\mathbf{H}}^*(\mathbf{x},t)=\mathbf{0}\,,\ \forall\mathbf{x}\in\Omega\,,\quad\forall t\,. \tag{2.14}$$

The variational setting provides the weak form of the Fourier's equation, where the variation of (2.13), i.e., $-\nabla\cdot\delta\mathbf{H}^+(\mathbf{x},t) = c\ \delta\theta(\mathbf{x},t)$, is used as a holonomic constrain. The counterpart of (2.11) now reads (Biot, 1970)

$$\int_\Omega c\ \theta(\mathbf{x},t)\ \delta\theta\ dV + \int_\Omega \frac{1}{\lambda}\ \dot{\mathbf{H}}^+(\mathbf{x},t)\ \delta\mathbf{H}^+\ dV = -\int_\Omega \frac{1}{\lambda}\ \dot{\mathbf{H}}^*(\mathbf{x},t)\ \delta\mathbf{H}^+\ dV - \int_{\partial\Omega}\theta(\mathbf{x},t)\ \delta\mathbf{H}^+\cdot\mathbf{n}\ ds\,. \tag{2.15}$$

This formulation is amenable of a straightforward finite element implementation in space.

We remark that, by comparing Eqs. (2.11) and (2.15), the two variational settings coincide when there are no heat generation/absorption, i.e., $\mathbf{H}^*(\mathbf{x},t)=\mathbf{H}^\sharp(\mathbf{x},t)=0$, and consequently $\mathbf{H}^+(\mathbf{x},t)=\mathbf{H}(\mathbf{x},t)=0$. Moreover, the initial temperature $\theta_0(\mathbf{x})$ does not appear in the expression proposed by Biot (1970). This is not a problem because only the variation of the energy conservation law is used as an internal constraint. In any case, for the definition of the "neat" form of the principle, it is useful to preserve the physical interpretation of the heat displacement, as defined in Section 2.1.

2.3. The "neat" formulation of the variational principle

Following the definition (2.6) of the heat displacement fields $\mathbf{H}(\mathbf{x},t)$ and $\mathbf{H}^\sharp(\mathbf{x},t)$, the weak form of the energy conservation law (2.8) can be obtained by multiplying the expression (2.8) by the variation $\nabla\cdot\delta\mathbf{H}$, i.e.,

$$\int_\Omega \left[\theta(\mathbf{x},t)-\theta_0(\mathbf{x})\right]\nabla\cdot\delta\mathbf{H}\ dV + \int_\Omega \frac{1}{c}\ \nabla\cdot\left[\mathbf{H}(\mathbf{x},t)+\mathbf{H}^\sharp(\mathbf{x},t)\right]\ \nabla\cdot\delta\mathbf{H}\ dV = 0\,. \tag{2.16}$$

The field $\mathbf{H}(\mathbf{x},t)$ is required to be continuous, whereas its variation $\delta\mathbf{H}$ shall satisfy the boundary conditions. Using the divergence theorem and considering Fourier's law (2.1), the first term can be written as

$$\begin{aligned}&\int_\Omega \left[\theta(\mathbf{x},t)-\theta_0(\mathbf{x})\right]\nabla\cdot\delta\mathbf{H}\ dV = \\ &\quad\int_\Omega \frac{1}{\lambda}\ \dot{\mathbf{H}}(\mathbf{x},t)\cdot\delta\mathbf{H}\ dV + \int_{\partial\Omega}\theta(\mathbf{x},t)\ \delta\mathbf{H}\cdot\mathbf{n}\ ds - \int_\Omega \theta_0(\mathbf{x})\nabla\cdot\delta\mathbf{H}\ dV\,,\end{aligned} \tag{2.17}$$

so that (2.16) may be rearranged in the form

$$\begin{aligned}&\int_\Omega \frac{1}{c}\ \nabla\cdot\mathbf{H}(\mathbf{x},t)\ \nabla\cdot\delta\mathbf{H}\ dV + \int_\Omega \frac{1}{\lambda}\ \dot{\mathbf{H}}(\mathbf{x},t)\cdot\delta\mathbf{H}\ dV = \\ &\quad-\int_{\partial\Omega}\theta(\mathbf{x},t)\delta\mathbf{H}\cdot\mathbf{n}\ ds + \int_\Omega \theta_0(\mathbf{x})\nabla\cdot\delta\mathbf{H}\ dV - \int_\Omega \frac{1}{c}\ \nabla\cdot\mathbf{H}^\sharp(\mathbf{x},t)\ \nabla\cdot\delta\mathbf{H}\ dV\,.\end{aligned} \tag{2.18}$$

Observe that only the divergence of $\mathbf{H}^\sharp(\mathbf{x},t)$ appears in this expression. From (2.6b), this is the amount of heat generated/absorbed in the volume up to the current time.

The final form of the variational principle can be obtained from (2.18) with the divergence theorem, i.e.,

$$\int_{\Omega} \left\{ -\frac{1}{c}\nabla \left[\nabla \cdot \left[\mathbf{H}(\mathbf{x},t) + \mathbf{H}^{\sharp}(\mathbf{x},t) \right] \right] + \frac{1}{\lambda}\dot{\mathbf{H}}(\mathbf{x},t) + \nabla\theta_0(\mathbf{x}) \right\} \cdot \delta\mathbf{H} \, dV + \int_{\partial\Omega} \left\{ \theta(\mathbf{x},t) - \theta_0(\mathbf{x}) + \frac{1}{c}\nabla \cdot \left[\mathbf{H}(\mathbf{x},t) + \mathbf{H}^{\sharp}(\mathbf{x},t) \right] \right\} \delta\mathbf{H} \cdot \mathbf{n} \, ds = 0 \,. \tag{2.19}$$

Remarkably, this formulation involves only the heat flux, whereas the temperature only appears at the boundary.

The arbitrariness of the variation $\delta\mathbf{H}$ inside the body provides the strong form of governing field equation, i.e.,

$$\frac{1}{\lambda}\dot{\mathbf{H}}(\mathbf{x},t) = \nabla \left[\frac{1}{c}\nabla \cdot \left[\mathbf{H}(\mathbf{x},t) + \mathbf{H}^{\sharp}(\mathbf{x},t) \right] - \theta_0(\mathbf{x}) \right] \,, \quad \forall \mathbf{x} \in \Omega, \quad \forall t \,, \tag{2.20}$$

which has to be solved under appropriate boundary conditions, detailed in Section 2.4.

Suppose that $\mathbf{H}(\mathbf{x},t)$ has been found. The temperature field in the body can be obtained by using Fourier's law (2.1) as a constraint, which provides $\frac{1}{\lambda}\dot{\mathbf{H}}(\mathbf{x},t) = -\nabla\theta(\mathbf{x},t)$. Therefore, any heat displacement and temperature field which contemporaneously satisfies (2.1) and (2.20) shall be such that

$$-\nabla\theta(\mathbf{x},t) = \nabla \left[\frac{1}{c}\nabla \cdot \left[\mathbf{H}(\mathbf{x},t) + \mathbf{H}^{\sharp}(\mathbf{x},t) \right] - \theta_0(\mathbf{x}) \right] \,, \quad \forall \mathbf{x} \in \Omega \,, \quad \forall t \,. \tag{2.21}$$

This implies that $\theta(\mathbf{x},t) - \theta_0(\mathbf{x}) + \frac{1}{c}\nabla \cdot \left[\mathbf{H}(\mathbf{x},t) + \mathbf{H}^{\sharp}(\mathbf{x},t) \right] = F(t)$, i.e., it is a function of time only, being its gradient null in the whole domain.

When the variation $\delta\mathbf{H}\cdot\mathbf{n}$ is not zero on a part $\partial_p\Omega$ of the boundary $\partial\Omega$, the natural boundary condition provided by the boundary term of (2.19) readily implies that

$$\theta(\mathbf{x},t) - \theta_0(\mathbf{x}) + \frac{1}{c}\nabla \cdot \left[\mathbf{H}(\mathbf{x},t) + \mathbf{H}^{\sharp}(\mathbf{x},t) \right] = F(t) = 0 \,, \quad \forall \mathbf{x} \in \partial_p\Omega \,, \quad \forall t \,. \tag{2.22}$$

Therefore, one obtains $F(t) = 0$ in the whole domain Ω and, consequently,

$$\theta(\mathbf{x},t) - \theta_0(\mathbf{x}) + \frac{1}{c}\nabla \cdot \left[\mathbf{H}(\mathbf{x},t) + \mathbf{H}^{\sharp}(\mathbf{x},t) \right] = 0 \,, \quad \forall \mathbf{x} \in \Omega \,, \quad \forall t \,. \tag{2.23}$$

This is the energy conservation law (2.8). The case in which $\delta\mathbf{H} \cdot \mathbf{n} = 0$ on the whole boundary $\partial\Omega$ deserves a particular attention, because it entails an intrinsic indeterminacy in the temperature field $\theta(\mathbf{x},t) - \theta_0(\mathbf{x})$. It will be considered as case (ii) in the next Section 2.4.

We take the liberty to call this variational formulation "neat" in comparison with the "classical" one, described in Section 2.2, because it has the noteworthy advantage that it involves only the heat displacement as the unknown field. This is very useful in the numerical implementation, as it will be discussed in Section 3. It considers Fourier's law as a constraint and provides the energy conservation law via the Euler–Lagrange equations; the vice-versa occurred in the "classical" formulation.

Remark 2.2 (*A Mechanical Interpretation à la Biot*)**.** Following Biot (1970), the terms on the left-hand-side of (2.18) can be interpreted as the variation of the *thermal potential* $\mathcal{V}_H$, associated with the heat flowing into the volume, and of the *dissipation function* $\mathcal{D}$, defined as

$$\delta\mathcal{V}_H := \int_{\Omega} \frac{1}{c} \, \nabla \cdot \mathbf{H}(\mathbf{x},t) \, \nabla \cdot \delta\mathbf{H} \, dV \,, \tag{2.24a}$$

$$\delta\mathcal{D} = \int_{\Omega} \frac{1}{\lambda} \, \dot{\mathbf{H}}(\mathbf{x},t) \, \delta\mathbf{H} \, dV \,. \tag{2.24b}$$

The terms on the right-hand-side indicate the *thermal driving forces*

$$\delta\mathcal{Q} := -\int_{\partial\Omega} \theta(\mathbf{x},t) \, \delta\mathbf{H} \cdot \mathbf{n} \, ds \,, \tag{2.25a}$$

$$\delta\mathcal{Q}_0 := \int_{\Omega} \theta_0(\mathbf{x}) \nabla \cdot \delta\mathbf{H} \, dV \,, \tag{2.25b}$$

$$\delta\mathcal{Q}^{\sharp} := -\int_{\Omega} \frac{1}{c} \, \nabla \cdot \mathbf{H}^{\sharp}(\mathbf{x},t) \, \nabla \cdot \delta\mathbf{H} \, dV \,. \tag{2.25c}$$

In particular, $\delta\mathcal{Q}_0$ and $\delta\mathcal{Q}^{\sharp}$ indicate the contributions respectively due to the initial temperature distribution and the energy generated in the volume, whereas $\delta\mathcal{Q}$ accounts for the effect of the temperature distribution at the domain boundaries. Notice that the temperatures at the domain boundaries and the volume heat source may be time-dependent. From (2.24) and (2.25), the variational principle (2.18) can be written as

$$\delta\mathcal{V}_H + \delta\mathcal{D} = \delta\mathcal{Q} + \delta\mathcal{Q}_0 + \delta\mathcal{Q}^{\sharp} \,. \tag{2.26}$$

This notation has a mechanical analogy with the equations that regulate the motion of an elastic system with viscous dissipation and negligible mass. This is obtained through the definition of the variation of a Rayleigh-type dissipation function, which includes the effects of velocity-proportional dissipative forces in the energy equations (Euler–Lagrange) of a classical mechanical system (Bersani & Caressa, 2021; Nguyen, 1994; Virga, 2015).

Remark 2.3 (*The "Neat" Variational Principle in Biot's Notation*)**.** The "neat" variational principle can be re-stated in terms of the Biot's heat displacement fields $\mathbf{H}^+(\mathbf{x},t)$ and $\mathbf{H}^*(\mathbf{x},t)$, defined in Remark 2.1. For this, multiply the energy conservation law (2.13) by the variation $\nabla\cdot\delta\mathbf{H}^+$, and integrate it over the spatial domain Ω, to obtain

$$\int_\Omega \left[\theta(\mathbf{x},t)-\theta_0(\mathbf{x})\right]\nabla\cdot\delta\mathbf{H}^+\,dV+\int_\Omega\frac{1}{c}\,\nabla\cdot\mathbf{H}^+(\mathbf{x},t)\nabla\cdot\delta\mathbf{H}^+\,dV=0\,. \tag{2.27}$$

By considering Fourier's law (2.14), and integrating by parts, Eq. (2.27) may be rewritten as

$$\begin{aligned}&\int_\Omega\frac{1}{c}\,\nabla\cdot\mathbf{H}^+(\mathbf{x},t)\,\nabla\cdot\delta\mathbf{H}^+\,dV+\int_\Omega\frac{1}{\lambda}\dot{\mathbf{H}}^+(\mathbf{x},t)\cdot\,\delta\mathbf{H}^+\,dV=\\&-\int_{\partial\Omega}\theta(\mathbf{x},t)\delta\mathbf{H}\cdot\mathbf{n}\,ds+\int_\Omega\theta_0(\mathbf{x})\nabla\cdot\delta\mathbf{H}\,dV-\int_\Omega\frac{1}{\lambda}\dot{\mathbf{H}}^*(\mathbf{x},t)\cdot\,\delta\mathbf{H}^+\,dV\,.\end{aligned} \tag{2.28}$$

Again, it can be verified that, when there are no heat generation/absorption, i.e., $\mathbf{H}^*(\mathbf{x},t)=\mathbf{H}^\sharp(\mathbf{x},t)=0$, this expression coincides with (2.18).

The so obtained variational formulation is not *complementary* to the classical Biot's setting presented in Remark 2.1, since the variable subjected to variation is, again, the heat displacement field. However, it may be considered *dual* because what is inverted is the role of the expressions (2.1) and (2.3) as "constraint" and "Euler–Lagrange equation".

2.4. Boundary conditions and temperature field

Through the "neat" variational principle (2.18), one can find the heat displacement field $\mathbf{H}(\mathbf{x},t)$. The temperature field can be recovered *a posteriori*, from the internal constraint (2.1), which can be written as

$$\nabla\cdot\dot{\mathbf{H}}(\mathbf{x},t)=-\lambda\,\Delta\theta(\mathbf{x},t)\,,\quad\forall\mathbf{x}\in\Omega\,,\quad\forall t\,. \tag{2.29}$$

This is Poisson's equation, which allows to determine $\theta(\mathbf{x},t)$ from the conditions that this field has to satisfy on the boundary.

In most thermal problems, the boundary conditions are usually of three types (Lienhard & Lienhard, 2019; Mills, 1992).

i. The (possibly time-dependent) temperature $\overline{\theta}(\mathbf{x},t)$ is specified on the domain boundary $\partial\Omega$. This value can be used in the variational Eq. (2.18). Observe that the value of $\delta\mathbf{H}\cdot\mathbf{n}$ is not constrained at the boundary, since (2.22) only determines the value of the divergence of $\mathbf{H}(\mathbf{x},t)$ at the boundary. Once $\mathbf{H}(\mathbf{x},t)$ and $\dot{\mathbf{H}}(\mathbf{x},t)$ are evaluated by solving the variational problem, the temperature field is determined from (2.29), with *Dirichlet* boundary conditions

$$\theta(\mathbf{x},t)=\overline{\theta}(\mathbf{x},t)\,,\qquad\forall\mathbf{x}\in\partial\Omega\,,\quad\forall t\,. \tag{2.30}$$

ii. The heat flux $\dot{\mathbf{H}}(\mathbf{x},t)\cdot\mathbf{n}=\dot{\bar{H}}_n(\mathbf{x},t)$ is specified on $\partial\Omega$. Integrating in time, this provides that $\mathbf{H}(\mathbf{x},t)\cdot\mathbf{n}=\bar{H}_n(\mathbf{x},t)$ is assigned for any t on $\partial\Omega$ and, consequently, the variation $\delta\mathbf{H}\cdot\mathbf{n}$ vanishes on the boundary. This implies that in the variational Eq. (2.19) the boundary integral disappears. The variational problem is solved under the requirement that $\mathbf{H}(\mathbf{x},t)\cdot\mathbf{n}$ is assigned on $\partial\Omega$, and the whole heat displacement field is found. The temperature field is found from (2.29) with boundary conditions of the *Neumann* type which, from the Fourier's law constraint, take the form

$$-\lambda\nabla\theta(\mathbf{x},t)\cdot\mathbf{n}=-\lambda\,\frac{\partial\theta(\mathbf{x},t)}{\partial\mathbf{n}}=\dot{\bar{H}}_n(\mathbf{x},t)\,,\quad\forall\mathbf{x}\in\partial\Omega\,,\quad\forall t\,. \tag{2.31}$$

It is clear that there is an intrinsic indeterminacy in the temperature field for this case. For example, if the thermal equations are satisfied by $\theta(\mathbf{x},t)$, they are also satisfied by $\theta(\mathbf{x},t)+\theta_1(t)$, obtained by adding the arbitrary uniformly distributed field $\theta_1(t)$. This is not surprising, since there are many ways to inject a prescribed heat flux from the boundary, as a function of the body temperature. In other words, knowledge of the heat sources and the heat fluxes on the whole boundary can only determine the gradients of the temperature fields at each time.

This is the only case in which variational principle cannot provide, *per se*, a unique solution in terms of temperature. To solve the indeterminacy, the energy conservation law (2.22) should be artificially considered on at least part of the boundary, even if it does not result from the variational form as a natural boundary conditions.

iii. *Robin conditions*, or boundary conditions of the third kind, are prescribed for the temperature field. In this case, the heat flux is proportional to the difference between the temperature at the boundary and the temperature of the surrounding medium $\theta_e(\mathbf{x},t)$, possibly dependent on time and the point $\mathbf{x}\in\partial\Omega$, according to an expression of the form

$$-\dot{H}_n(\mathbf{x},t)=\lambda\,\frac{\partial\theta(\mathbf{x},t)}{\partial\mathbf{n}}=h\left[\theta_e(\mathbf{x},t)-\theta(\mathbf{x},t)\right]\,,\quad\forall\mathbf{x}\in\partial\Omega\,,\quad\forall t\,, \tag{2.32}$$

where h is the surface heat transfer coefficient.[1] In this case, $\theta_e(\mathbf{x},t)$ is the boundary datum, whereas $\theta(\mathbf{x},t)$ is free. This implies that the boundary term in (2.19) can be written as

$$\begin{aligned}&\int_{\partial\Omega}\left\{\theta(\mathbf{x},t)-\theta_0(\mathbf{x})+\frac{1}{c}\nabla\cdot\left[\mathbf{H}(\mathbf{x},t)+\mathbf{H}^\sharp(\mathbf{x},t)\right]\right\}\delta\mathbf{H}\cdot\mathbf{n}\,ds\\&=\int_{\partial\Omega}\left\{\frac{1}{h}\dot{\mathbf{H}}(\mathbf{x},t)\cdot\mathbf{n}+\theta_e(\mathbf{x},t)-\theta_0(\mathbf{x})+\frac{1}{c}\nabla\cdot\left[\mathbf{H}(\mathbf{x},t)+\mathbf{H}^\sharp(\mathbf{x},t)\right]\right\}\delta\mathbf{H}\cdot\mathbf{n}\,ds\,.\end{aligned} \tag{2.33}$$

[1] In the most general case, the convective heat transfer coefficient h may vary on the boundary, and be temperature-dependent. Furthermore, the surface heat transfer law (2.32) can account, even in an approximated way, for both convection heat exchange and infra-red radiation. An example is provided in Section 4.3.

Again, the boundary conditions are obtained since the variation $\delta\mathbf{H}\cdot\mathbf{n}$ is arbitrary.
Once $\mathbf{H}(\mathbf{x},t)$ is determined, the temperature field is found from (2.29) with the mixed boundary condition (2.32), correlating $\frac{\partial\theta(\mathbf{x},t)}{\partial\mathbf{n}}$ with $\theta(\mathbf{x},t)$ at the border. Also in this case, energy conservation (2.23) is naturally provided by the variational form of the equations.

Remark 2.4 (*Robin Conditions in Biot's Formalism*)**.** Following Biot (1970), the boundary conditions (2.32) are accounted for via the driving force $\delta\mathcal{Q}$ (2.25a) as

$$\begin{aligned}\delta\mathcal{Q}=-\delta\mathcal{D}_b+\delta\mathcal{Q}_b\,,\quad \text{with } \delta\mathcal{D}_b &:=\int_{\partial\Omega}\frac{1}{h}\,\dot{H}_n(\mathbf{x},t)\,\delta\mathbf{H}\cdot\mathbf{n}\,ds\,,\\ \delta\mathcal{Q}_b &:=-\int_{\partial\Omega}\theta_e(\mathbf{x},t)\,\delta\mathbf{H}\cdot\mathbf{n}\,ds\,,\end{aligned}\tag{2.34}$$

where $\delta\mathcal{D}_b$ is a *boundary dissipation function*, while $\delta\mathcal{Q}_b$ accounts for the influence of the environmental temperatures. Accounting for (2.34), the variational principle (2.26) may be written as

$$\delta\mathcal{V}+\delta\mathcal{D}+\delta\mathcal{D}_b=\delta\mathcal{Q}_b+\delta\mathcal{Q}_0+\delta\mathcal{Q}^\sharp\,,\tag{2.35}$$

where the various quantities are as defined in Remark 2.2.

Of course, the aforementioned conditions may be contemporaneously applied on different parts of the body boundary. In general, it is not straightforward to solve Poisson's equation (2.29), either analytically or numerically. However, in the finite element implementations, such conditions can be directly enforced in the discretized version of the thermal equations.

2.5. A mechanical analogy for the one-dimensional case

A mechanical analogy for the one-dimensional case may serve to illustrate the "neat" variational principle. The reference configuration Ω is now the 1D domain of length s, with coordinate $z\in[0,s]$. The temperature field $\theta(z,t)$ and the heat flux in z direction $\dot{H}(z,t)$ are related by the 1D counterpart of Fourier's law (2.1), which reads

$$\lambda\;\theta'(z,t)+\dot{H}(z,t)=0\,,\quad \forall\mathbf{z}\in[0,s]\,,\quad \forall t\,,\tag{2.36}$$

where $'$ denotes differentiation with respect to z. From the one dimensional version of (2.6), the energy conservation law (2.8) is written in the form

$$-[H'(z,t)+H^{\sharp\prime}(z,t)]=c[\theta(z,t)-\theta_0(z)]\,,\quad \forall z\in[0,s]\,,\quad \forall t\,.\tag{2.37}$$

By coupling Eqs. (2.36) and (2.37), the 1D counterpart of the heat diffusion Eq. (2.3) is readily obtained (Lienhard & Lienhard, 2019), and the dual variational principle (2.18) reads

$$\begin{aligned}\int_0^s\frac{1}{c}\,H'(z,t)\delta H'\,dz+\int_0^s\frac{1}{\lambda}\,\dot{H}(z,t)\delta H\,dz=\\ -\,[\theta(z,t)\delta H]_0^s+\int_0^s\theta_0(z)\delta H'\,dz-\int_0^s\frac{1}{c}\,H^{\sharp\prime}(z,t)\delta H'\,dz\,.\end{aligned}\tag{2.38}$$

The field equation and the boundary conditions may be evaluated analogously to the three dimensional case detailed in Section 2.3. The one-dimensional reduction of the three types of boundary conditions and the a posteriori evaluation of the temperature field follows the same arguments of Section 2.4.

The mechanical analogy consists in a linear elastic rod $z\in[0,s]$, with Young's modulus E and cross sectional area A. As indicated in Fig. 1, each infinitesimal segment of the bar, comprised between the cross sections at z and $z+\mathrm{d}z$, is connected to the ground by a dashpot with viscous constant $\eta\,\mathrm{d}z$, such to form a homogeneous array. Suppose that each point z where the dashpot is anchored undergoes the displacement $u^\sharp(z,t)$, positive if in the direction of positive z, and let $u(z,t)$ denote the elongation of the end points of the dashpot, so that $u^\sharp(z,t)+u(z,t)$ is the total displacement of the point z of the bar.

In the initial reference configuration, at $t=0$, the bar is subjected to distributed forces per unit length $f_0(z)$. Define

$$F_0(z):=\int_0^z f_0(\zeta)\,d\zeta+N_0\,,\tag{2.39}$$

such that $F_0(0)=N_0$ and $F_0(s)=\int_0^s f_0(\zeta)\,d\zeta+F_0(0)$ are the normal forces acting at the bar ends at $t=0$. Furthermore, as shown in Fig. 1, time-dependent *compression* forces $F(0,t)$ and $F(s,t)$ are applied at the bar ends.

The equilibrium equation for an infinitesimal segment comprised between the generic section z and $z+dz$ reads

$$EA\left[u''(z,t)+u^{\sharp\prime\prime}(z,t)\right]-\eta\dot{u}(z,t)-F_0'(z)=0\,,\tag{2.40}$$

with boundary conditions

$$\begin{aligned}EA\left[u'(0,t)+u^{\sharp\prime}(0,t)\right]&=-F(0,t)+F_0(0)\,,\\ EA\left[u'(s,t)+u^{\sharp\prime}(s,t)\right]&=-F(s,t)+F_0(s)\,.\end{aligned}\tag{2.41}$$

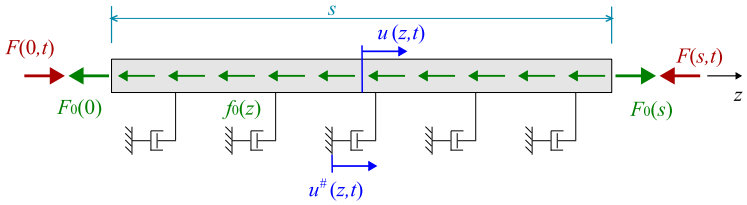

Fig. 1. Mechanical analogy for the one dimensional thermal problem: linear elastic bar connected to the ground by an array of dashpots.

To state the equivalence with the thermal problem, in which the temperature is prescribed at the boundary $z = 0$ and $z = s$, it is sufficient to set

$$EA = \frac{1}{c}, \quad \eta = \frac{1}{\lambda}. \tag{2.42}$$

From the analogy, it is evident that the displacement fields $u(z,t)$ and $u^\sharp(z,t)$ correspond to $H(z,t)$ and $H^\sharp(z,t)$, respectively, while $F_0(z)$ is the counterpart of the initial temperature $\theta_0(z)$.

More in particular, denoting with $N(z,t) = F(z,t) - F_0(z)$ the axial force in the bar, assumed positive if compressive, the constitutive law is in the form

$$N(z,t) = F(z,t) - F_0(z) = -EA\left[u'(z,t) + u^{\sharp\prime}(z,t)\right], \tag{2.43}$$

corresponding to the energy conservation law (2.37), while the axial equilibrium equation is

$$\eta\dot{u}(z,t) = -F'(z,t), \tag{2.44}$$

which is the counterpart of the Fourier's equation (2.36). Clearly, $F(z,t)$ corresponds to the temperature field $\theta(z,t)$. Hence, the compression forces $F(0,t)$ and $F(s,t)$ applied at the bar ends play the role of the boundary temperatures.

The condition (2.44) implies that any solution for which $\dot{u}(z,t) = 0$, such that $u(z,t) = u(z)$, shall be characterized by $F'(z,t) = 0$. This means that the heat flux is null: when the steady state condition is reached the temperature field is uniform. More generally, the analogy between the equations for the elastic and the thermal cases suggests that, in a finite element implementation of the thermoelastic problem, the same shape functions can be considered to approximate both the elastic and the heat displacements.

3. Finite element implementation

In Galuppi and Royer-Carfagni (2022), the one-dimensional version of the original variational principle by Biot, recalled in Remark 2.1, was numerically implemented by approximating the relevant fields with high order Hermite shape functions. Applications to multilayered plates composed of an arbitrary number of plies with different physical and thermal properties were provided. The implementation was extended in Galuppi and Royer-Carfagni (2023a, 2023b) to a three dimensional monolithic plate, unevenly irradiated on the surfaces, entailing periodic variation of the thermal driving forces. A major drawback is that compatible shape functions had to be assumed for the temperature and the heat displacement field, because they both enter in the fundamental variational principle. Remarkably, in the "neat" variational formulation only the displacement field needs to be considered.

3.1. Finite element discretization

The domain Ω is categorized in sub-domains, in each one of which the material is homogeneous. Each sub-domain is further divided into finite elements. The order of the variational form (2.38) indicates that the shape functions for the heat displacement field should entail at least C^0 continuity within each sub-domain and at the interface between the neighboring sub-domains. Henceforth, one can consider the nodal heat displacements as generalized time-dependent coordinates, and use simple tri-linear shape functions to interpolate the displacement field between the nodal points.

Let $\tilde{\mathbf{H}}(t)$ denote the vector collecting the $3N$ nodal values of the heat displacement, where N it the total number of nodes in the domain. Following standard procedures (Bathe, 2006; Zienkiewicz et al., 2005), the displacement field in a generic element e and in the whole body, respectively $\mathbf{H}_e(\mathbf{x},t)$ and $\mathbf{H}(\mathbf{x},t)$, are written as

$$\mathbf{H}_e(\mathbf{x},t) = \boldsymbol{\phi}(\mathbf{x})\,\tilde{\mathbf{H}}_e(t), \qquad \mathbf{H}(\mathbf{x},t) = \overline{\boldsymbol{\phi}}(\mathbf{x})\,\tilde{\mathbf{H}}(t), \tag{3.1}$$

where $\tilde{\mathbf{H}}_e(t)$ is the column vector containing $3n$ generalized coordinates, where n is the number of nodes in the element, while the $3 \times 3n$ matrix $\boldsymbol{\phi}(\mathbf{x})$ and the $3 \times 3N$ matrix $\overline{\boldsymbol{\phi}}(\mathbf{x})$ collect the shape functions, respectively for the element and for the whole body.

According to (3.1), the heat flux field and the variation of the heat displacement field in a generic element read

$$\dot{\mathbf{H}}_e(\mathbf{x},t) = \boldsymbol{\phi}(\mathbf{x})\,\dot{\tilde{\mathbf{H}}}_e(t)\,, \quad \delta\mathbf{H}_e(\mathbf{x},t) = \boldsymbol{\phi}(\mathbf{x})\,\delta\tilde{\mathbf{H}}_e(t)\,, \tag{3.2}$$

where $\delta\tilde{\mathbf{H}}_e(t)$ is the vector of the arbitrary variations of the generalized coordinates.

It is convenient to approximate the heat displacement field due to the heat source, $\mathbf{H}^\sharp(\mathbf{x},t)$, with the same shape functions used for $\mathbf{H}_e(\mathbf{x},t)$, such that $\mathbf{H}^\sharp_e(\mathbf{x},t) = \boldsymbol{\phi}(\mathbf{x})\ \tilde{\mathbf{H}}^\sharp_e(t)$ is the function at the element level; clearly, $\tilde{\mathbf{H}}^\sharp_e(t)$ is the column vector containing the nodal values of $\mathbf{H}^\sharp(\mathbf{x},t)$ at the considered element.

These approximations are used in the variational principle (2.19). For the generic element e, for which the constants c and λ are denoted by c_e and λ_e, one defines the quantities

$$\begin{aligned}
&\mathbf{K}_e := \frac{1}{c_e}\int_{\Omega_e}\left[\nabla^T\boldsymbol{\phi}(\mathbf{x})\right]^T\ \nabla^T\boldsymbol{\phi}(\mathbf{x})\ dV\,, \quad \mathbf{C}_e := \frac{1}{\lambda_e}\int_{\Omega_e}\boldsymbol{\phi}^T(\mathbf{x})\ \boldsymbol{\phi}(\mathbf{x})\ dV\,,\\
&\mathbf{q}_e(t) := -\int_{\partial\Omega_e}\theta(\mathbf{x},t)\ \boldsymbol{\phi}(\mathbf{x})\cdot\mathbf{n}\ ds\,, \quad \mathbf{q}_{0,e}(t) := \int_{\Omega_e}\theta_0(\mathbf{x})\nabla^T\boldsymbol{\phi}(\mathbf{x})\ dV\,,\\
&\mathbf{q}^\sharp_e(t) := -\frac{1}{c_e}\int_{\Omega_e}\nabla\cdot\mathbf{H}^\sharp(\mathbf{x},t)\ \nabla^T\boldsymbol{\phi}(\mathbf{x})\ dV = -\mathbf{K}_e\tilde{\mathbf{H}}^\sharp_e(t)\,,
\end{aligned} \tag{3.3}$$

where $\mathbf{q}_e(t)$, $\mathbf{q}_{0,e}(t)$ and $\mathbf{q}^\sharp_e(t)$ are the counterpart of the thermal driving forces defined by (2.25). At the element level, one finds from (2.19) the matrix form (Biot, 1970; Galuppi & Royer-Carfagni, 2022, 2023a)

$$\mathbf{K}_e\,\tilde{\mathbf{H}}_e(t) + \mathbf{C}_e\,\dot{\tilde{\mathbf{H}}}_e(t) = \mathbf{q}_e(t) + \mathbf{q}_{0,e} - \mathbf{K}_e\tilde{\mathbf{H}}^\sharp_e(t)\,, \tag{3.4}$$

where $\mathbf{K}_e$ and $\mathbf{C}_e$ play the role of element stiffness and damping $(3n\times 3n)$ matrices, respectively.

Following the classical direct assembly method (Zienkiewicz et al., 2005), the matrix form on the full domain reads

$$\mathbf{K}\,\tilde{\mathbf{H}}(t) + \mathbf{C}\,\dot{\tilde{\mathbf{H}}}(t) = \mathbf{q}(t) + \mathbf{q}_0 - \mathbf{K}\tilde{\mathbf{H}}^\sharp(t)\,, \tag{3.5}$$

where the global $\mathbf{K}$ and $\mathbf{C}$ $(3N\times 3N)$ matrices are band matrices.

Notice that the term $\mathbf{q}_e(t)$ in (3.4) accounts for the temperatures at the element boundaries. Unless an interfacial thermal resistance is present, a case which will be specifically considered in Section 3.3, the matching conditions of the variational principle, derived from the continuity of the heat displacement and its variation, imply that the temperature field is continuous. Thanks to this, all the terms cancel out after assembling the $\mathbf{q}_e(t)$ vectors, except on the external domain boundary $\partial\Omega$. The only surviving term is

$$\mathbf{q}(t) = -\int_{\partial\Omega}\theta(\mathbf{x},t)\ \boldsymbol{\phi}(\mathbf{x})\cdot\mathbf{n}\ ds\,. \tag{3.6}$$

This is analogous to the elimination of internal nodal forces via virtual work, a standard result in Finite Element (FE) approach (Zienkiewicz et al., 2005) that can also be verified through the "interconnection principle" established by Biot (1970).

Once $\tilde{\mathbf{H}}(t)$ is found by solving (3.5) with proper boundary conditions, the temperature field $\theta(\mathbf{x},t)$ can be evaluated by integrating Fourier's equation (2.1), as indicated in Section 2.4. The integration constants in space can be found from the boundary conditions, while the time integration constant comes from the initial conditions on the temperature field.

The proposed FE approach can be particularized to two- and one-dimensional problems, by reducing the number of degrees of freedom associated to each node. Examples of one-dimensional applications will be provided in Sections 4.1 and 4.2.

3.2. Boundary conditions

The numerical implementation of the boundary conditions of Section 2.4 is as follows.

i. When temperatures are prescribed at the boundaries, one evaluates the vector $\mathbf{q}(t)$ of the thermal driving forces by considering the (possibly space- and time-dependent) prescribed temperatures.
ii. When the normal component of the heat flux is prescribed at a boundary, the correspondent nodal values of $\dot{\tilde{\mathbf{H}}}(t)$ in (3.5) and, consequently, of $\tilde{\mathbf{H}}(t)$, can be obtained. Since the variation of the heat flux is null, the boundary term in (2.18) disappears; consequently, the terms of $\mathbf{q}(t)$ in (3.6) which are associated with the considered boundary degrees of freedom, are set equal to zero. In the particular case of perfect insulation, a null heat flux is prescribed: the corresponding degrees of freedom can be set to zero, which is equivalent to reducing the number of equations in (3.5).
iii. When boundary temperatures are given functions of the environmental temperatures and of the heat flux (Robin conditions), one can substitute the value of the temperature as a function of $\dot{H}_n$ and the external temperature in the boundary term of (2.19). To make the calculation explicit, consider the boundary conditions in the form (2.32). Solving for $\theta(\mathbf{x},t)$ and substituting in the boundary term of (2.19), using the discretization (3.1), one finds that (3.5) becomes

$$\mathbf{K}\,\tilde{\mathbf{H}}(t) + \left[\mathbf{C}+\mathbf{C}_b\right]\,\dot{\tilde{\mathbf{H}}}(t) = \mathbf{q}_b(t) + \mathbf{q}_0 - \mathbf{K}\tilde{\mathbf{H}}^\sharp(t)\,, \tag{3.7}$$

where

$$\mathbf{C}_b := \frac{1}{h}\int_{\partial\Omega} \boldsymbol{\phi}^T(\mathbf{x})\ \boldsymbol{\phi}(\mathbf{x})\cdot\mathbf{n}\ ds\,, \tag{3.8a}$$

$$\mathbf{q}_b(t) = -\int_{\partial\Omega} \theta_e(\mathbf{x},t)\ \boldsymbol{\phi}(\mathbf{x})\cdot\mathbf{n}\ ds\,. \tag{3.8b}$$

Observe that the term associated with $\mathbf{C}_b$ accounts for *boundary dissipation* (Biot, 1970).

3.3. Interfacial thermal resistance

Layers with different physical and thermal properties, widely used in many applications (Pásztory & Le Duong, 2021; Sadineni, Madala, & Boehm, 2011), can be considered by using the corresponding values for λ_e and c_e in the element stiffness and damping matrices (3.3). There is no need of implementing particular interface conditions, apart from the continuity of the heat flux.

A particular case is that of an *Interfacial Thermal Resistance* (ITR), also known as *thermal contact resistance* or *Kapitza resistance* (Ruan, Shi, Guo, & Gu, 2020). This is the resistance to heat flow at the interface between two materials, arising from the combination of poor mechanical or chemical adherence at the interface and/or thermal expansion mismatch (Benveniste & Miloh, 1986; Lipton & Vernescu, 1996; Nan, Birringer, Clarke, & Gleiter, 1997), and it is specifically relevant for solid–gas and solid–liquid interfaces (Chen, Xu, Zhou, & Li, 2022; Liang & Hu, 2018). The result is a jump in the temperature profile, proportional to the heat flux normal to the interface (Chen et al., 2022; Yuan, Yu, Li, & Fang, 2022).

To illustrate, consider the case where the ITR is a smooth surface $\partial\Omega_{ITR}$. Introduce a local orthogonal curvilinear system of coordinates (ξ,η,ζ), with arclength parametrization, such that $\partial\Omega_{ITR}$ corresponds to $\zeta = 0$, the axis ζ is orthogonal to $\partial\Omega_{ITR}$, whereas the axes associated with the ξ and η lines are tangent to $\partial\Omega_{ITR}$. The heat flux across the interface in the direction of ζ is

$$\dot{H}_\zeta(\xi,\eta,0,t) = -\frac{1}{R}\left[\theta(\xi,\eta,0^+,t) - \theta(\xi,\eta,0^-,t)\right]\,, \tag{3.9}$$

where R is the value of the interfacial thermal resistance and $\theta(\xi,\eta,0^\pm,t)$ represent the temperatures on the two sides of the interface.

In the proposed approach, this contribution affects the dissipation term in (2.19), i.e., the one where the coefficient $1/\lambda$ appears. One can interpret the resistant interface as a thermally *anisotropic* ply, as per (Biot, 1970), of very small thickness $\Delta\zeta$, i.e., $\zeta \in \left(-\frac{1}{2}\Delta\zeta, \frac{1}{2}\Delta\zeta\right)$, and very low thermal conductivity λ_ζ in the ζ direction. There are no internal heat sources, no heat is stored,[2] so that the heat fluxes, assuming that $\Delta\zeta$ is very small, are uniform in the ζ direction. Consequently, from (2.1), the temperature is linearly distributed in the thickness.

Now, consider the limit for $\Delta\zeta \to 0$ and $\lambda_\zeta \to 0$, while $\Delta\zeta/\lambda_\zeta \to R$. Therefore, the contribution in the dissipative term of (2.18) reads

$$\lim_{\Delta\zeta\to 0}\ \frac{1}{\lambda_\zeta}\int_{\partial\Omega_{ITR}}\int_{-\Delta\zeta/2}^{\Delta\zeta/2} \dot{H}_\zeta(\xi,\eta,\zeta,t)\,\delta H_\zeta\ d\zeta\ dA = R\int_{\partial\Omega_{ITR}} \dot{H}_\zeta(\xi,\eta,0,t)\,\delta H_\zeta\ dA\,. \tag{3.10}$$

In the numerical implementation, the ITR is considered by placing nodes in correspondence of the interface. The matrix form (3.5) of the variational principle becomes

$$\mathbf{K}\,\tilde{\mathbf{H}}(t) + \left[\mathbf{C} + \mathbf{C}_{ITR}\right]\,\dot{\tilde{\mathbf{H}}}(t) = \mathbf{q}(t) + \mathbf{q}_0 - \mathbf{K}\tilde{\mathbf{H}}^\sharp(t)\,, \tag{3.11}$$

where $\mathbf{C}_{ITR}$ is a square matrix, where the only non-zero terms are those corresponding to the degrees of freedom associated with $\dot{H}_\zeta(\xi,\eta,\zeta,t)$ of the interfacial nodes, which are equal to R.

4. Examples and comparisons

Two one-dimensional examples are first proposed as benchmark problems, since their solution was obtained by other authors with a different approach. Here, Ω is the 1D domain $z \in [0,s]$. Each node used for the discretization of the 1D heat displacement $H_z(z,t)$ has one degree of freedom, so that the shape function matrices $\boldsymbol{\phi}(\mathbf{x})$ and $\overline{\boldsymbol{\phi}}(\mathbf{x})$ collapse into vectors. Once the nodal values are found from (3.5), the temperature is determined by direct 1D integration of Fourier's law (2.1), with constants of integration in each element derived from the boundary conditions and continuity at the nodes; in the case of ITR, the jump is determined by the heat flux via (3.9). Alternatively, following a common procedure in FEM (Bathe, 2006; Zienkiewicz et al., 2005), the *nodal temperatures* can be directly recovered as the internal forces on each node: once $\tilde{\mathbf{H}}_e(t)$ and $\dot{\tilde{\mathbf{H}}}_e(t)$ are known, Eq. (3.4) can be inverted to find $\mathbf{q}_e(t)$. It has been verified that the two approaches give identical results. A three-dimensional example is proposed in Section 4.3. The FE model has been implemented by using the GiD program (Coll et al., 2018) to pre-process the input data.

The chosen examples are paradigmatic benchmark problems. Example 1 reproduces a classical problem, already considered by Biot (1970); example 2 concerns an interfacial thermal resistance; example 3 considers differently irradiated regions in layered composites. Both examples 2 and 3 typically involve high temperature gradients.

[2] This is equivalent (Yuan et al., 2022) to assume that $c = 0$ in (2.3).

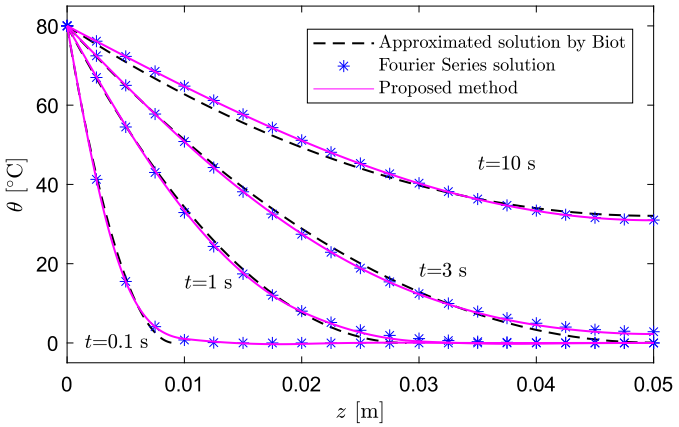

Fig. 2. Example 1. Temperature profile at different times evaluated with the proposed approach, compared with Biot's solutions (Biot, 1970), and with the solution of the differential form of the thermal problem obtained in Fourier series expansion (Carslaw & Jaeger, 1947).

4.1. Example 1 - Plate with prescribed temperature at one face and insulated at the other

This 1D example was originally proposed by Biot (1957, 1970). It regards a homogeneous pane of thickness $s = 50\,\text{mm}$, initially at the uniform temperature $\theta_0(z) = 0\ ^\circ\text{C}$. At $t = 0$, the face $z = 0$ is suddenly brought to the temperature $80\ ^\circ\text{C}$, while the face $z = s$ is thermally insulated. No heat sources are present. This corresponds to boundary conditions of the first and the second kind, according to the definitions of Sections 2.4 and 3.2, i.e.,

$$\theta(0,t) = \overline{\theta} = 80\ ^\circ\text{C}\,, \qquad \dot{H}(s,t) = 0\,, \quad \forall t\,. \tag{4.1}$$

Biot solved the problem (Biot, 1970) approximating the temperature field with parabolic functions, by dividing the heating process into two phases. First, heat penetrates up to a depth $z = \bar{s}$, called *penetration depth*. This phase ends at $t = \bar{t}$, when the penetration depth equals the plate thickness ($\bar{s} = s$). In the second phase, for $t > \bar{t}$, the temperature rises at the insulated boundary.

In our numerical solution, the mesh is refined in the neighborhood of $z = 0$ since the temperature presents here a discontinuity at $t = 0$: 20 elements, 0.5 mm thick, are used for $0 < z < 10\,\text{mm}$, while 8 elements, 5 mm thick, compose the remaining part.

The obtained results in terms of temperature profile $\theta(z,t)$ at different t, evaluated by setting $\lambda = 200\ \text{W/(m K)}$ and $c = 2.7 \cdot 10^6\ \text{J/(m}^3\ \text{K)}$, are plotted in Fig. 2. For the sake of comparison, the same figure shows Biot's solution (Biot, 1970), and the results obtained by solving the differential form of the heat conduction equations via Fourier series expansion (first 30 terms of the series), as in Carslaw and Jaeger (1947). The results show an excellent agreement.

4.2. Example 2 - Element with interfacial thermal resistance

This problem, proposed in Yuan et al. (2022), is that of a composite plate made of two layers of thickness $s_1 = s_2 = 0.5$ m, with $\lambda_1 = 200\ \text{W/(m K)}$, $\lambda_2 = 100\ \text{W/(m K)}$, and $c_1 = c_2 = 2.7 \cdot 10^6\ \text{J/(m}^3\ \text{K)}$, with an Interfacial Thermal Resistance $R = 1/500\ \text{m}^2\ \text{K/W}$. The initial temperature is assumed uniform and equal to $20\ ^\circ\text{C}$. At $t = 0$ the temperature is suddenly raised to $480\,^\circ\text{C}$ on the side $z = 0$, whereas it is kept fixed at $20\,^\circ\text{C}$ at $z = s_1 + s_2 = s$.

In Yuan et al. (2022), different 1D modeling strategies, solved with finite differences, were developed to account for the ITR: *(i)* numerically implement the ITR relation (3.9) in terms of the temperature derivative; *(ii)* create a "virtual layer" with a very small thermal conductivity λ_ζ (compare Eq. (3.10)) at the interface to represent the ITR; *(iii)* use a local "artificial layer" surrounding the interface with modified thermal properties, to reflect the influence of the ITR on the heat transfer through the interface. These approaches are reliable, but require a very fine mesh: by changing the mesh size, the temperature profile does change. The convergence is reached using 500 elements, 2 mm thick, with a time step of 0.001 h.

In the proposed variational approach, we have verified that convergence is reached with only 20 elements, 50 mm thick, with a time step of 0.01 h. Accurate results may be also be obtained with only four elements, but this mesh is not accurate for the evaluation of the interfacial temperatures in the first minutes of the "loading" history, when the temperature profile presents a high slope in proximity of the surface $z = 0$, where the temperature jump is instantaneous. Therefore, at the beginning of the transient state, a finer mesh is required to correctly reproduce the temperature profile. When the temperature profile smooths out as a consequence of heat conduction, a coarse mesh is sufficient for a good accuracy.

Fig. 3(a) shows a comparison of the temperature profiles at $t = 1500$ s, also recorded in Yuan et al. (2022), with evidence of the temperature jump at the ITR surface. Fig. 3(b) shows the time evolution of the temperatures on the two faces of the ITR, i.e., $\theta_{ITR,l}(t) = \theta(s_1^-, t)$ and $\theta_{ITR,r}(t) = \theta(s_1^+, t)$. The difference with the solution proposed in Yuan et al. (2022) is of the order of $0.5\,^\circ\text{C}$.

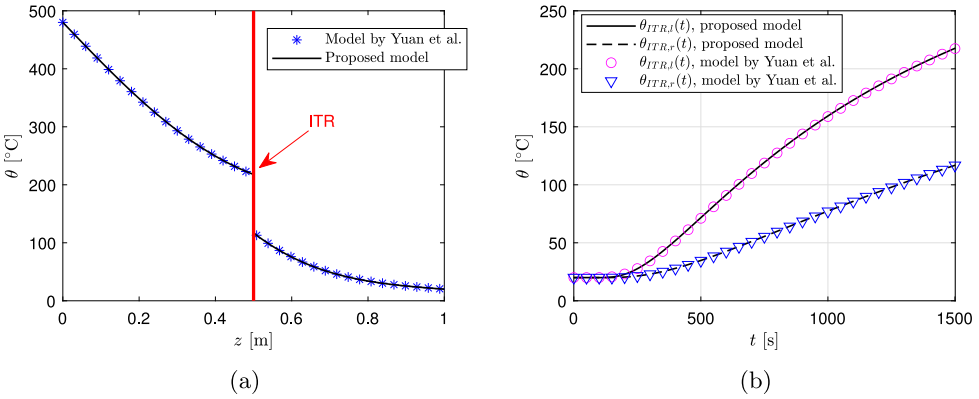

Fig. 3. Example 2. Comparison between the solution obtained with the proposed approach and that proposed by Yuan et al. (2022). (a) Temperature profile at $t = 1500\,\mathrm{s}$; (b) time evolution of the temperatures on the two faces of the ITR.

4.3. Example 3 - Partially shaded laminated glass pane

The third, 3D, example is representative of a window glass pane, unevenly irradiated by the sun due to cast shadows on its surface, which separates environments at different temperature. At $t = 0$ the temperature of pane is supposed to be uniform; at $t = 0^+$ the body is put in contact with the environments and is (unevenly) irradiated by the sun. We calculate the transient thermal state, until the steady-state condition is reached. The model could also account for seasonal- or daily-varying boundary conditions, but this analysis is not done here.

Table 1
Values of physical and thermal properties for the materials considered in Example 3.

Material	Reference	c [J/(m^3 K)]	λ [W/(m K)]	α [–]	τ [–]
Glass	EN (2012) and N180E (2004)	1800 10^3	1	0.23	0.67
PVB	Alvarez, Flores, and Estrada (1998) and Carrot, Bendaoud, Pillon, Olabisi, and Adewale (2016)	1478.3 10^3	0.236	0.01	0.99

Consider the 1 m × 1.5 m rectangular laminated glass pane represented in Fig. 4, composed by alternating glass plies with PVB polymeric interlayer, with very different physical and thermal properties (Alvarez et al., 1998; Galuppi & Royer-Carfagni, 2022), as indicated in Table 1.

Here, according to a practice followed by most authors, it is assumed that the interfacial thermal resistance at the glass-PVB interface is negligible, even if the presence of an ITR cannot be ruled out a priori. According to Pietrak and Wisniewski (2014), the ITR effect is low in case of an efficient mechanical and chemical bond between the constituents, such as for well-made laminated glass. There are cases, however, in which partial delamination occurs, due to poor manufacturing or exposure to an aggressive environment, for which the ITR would come into play.

A reference system is introduced, such that x, y are the in-plane directions and z is along the thickness. The panel is defined by $0 \le x \le 1.0\,\mathrm{m}$, $0 \le y \le 1.5\,\mathrm{m}$. The laminate is made of one glass ply ($0 < z < s_1$) of thickness $s_1 = 12\,\mathrm{mm}$, the PVB interlayer ($s_1 < z < s_1 + s_2$) of thickness $s_2 = 1.5\,\mathrm{mm}$, and the third glass ply ($s_1 + s_2 < z < s_1 + s_2 + s_3 = s$) of thickness $s_3 = 6\,\mathrm{mm}$. The shaded region is rectangular and identified by the domain $0 < x < 0.5\,\mathrm{m}$ and $0 < y < 0.5\,\mathrm{m}$.

As shown in Fig. 4, the panel is discretized by using one element in the thickness for each layer (three elements in total), and by dividing the surface into 30 and 50 elements respectively in the x and y directions (4500 elements and 6324 nodes). The mesh is refined in the neighborhood of the interface between shaded and unshaded regions, where conduction heat exchange occurs. Tri-linear shape functions have been used.

The panel exchanges heat via convection (with the external and the internal air) and radiation (with the sky vault and external surfaces (ISO, 2003), and with other internal surfaces (Marino, Nucara, Pietrafesa, & Polimeni, 2017) assumed to be at the same temperature θ_i of the internal air (EN, 2007)). Although the radiant energy exchange is proportional to the fourth power of the absolute temperatures (Lardner, 1963), since the temperature difference between panel and environment is small, the expressions can be linearized (Lienhard & Lienhard, 2019). The conclusion is that all the heat-exchange contributions at the panel surfaces provide boundary conditions of the Robin kind (2.32). This can be written in the form

$$\dot{H}_z(x,y,0,t) = h_i\left[\theta_i - \theta(x,y,0,t)\right]\,, \quad \dot{H}_z(x,y,s,t) = h_e\left[\theta(x,y,s,t) - \theta_e\right]\,, \quad \forall t\,, \tag{4.2}$$

where h_e and h_i are the *total* heat transfer coefficient on the external and internal surfaces, respectively, simultaneously accounting for both convection and radiation, while θ_e is the "nominal" external temperature, defined so to provide the formal equivalence (Galuppi & Royer-Carfagni, 2022).

The solar radiation, here denoted as G, can be modeled as an internal heat source (Galuppi & Royer-Carfagni, 2022; Lienhard & Lienhard, 2019). The total density of heat flow rate depends on several factors, such as season, time of day, panel orientation

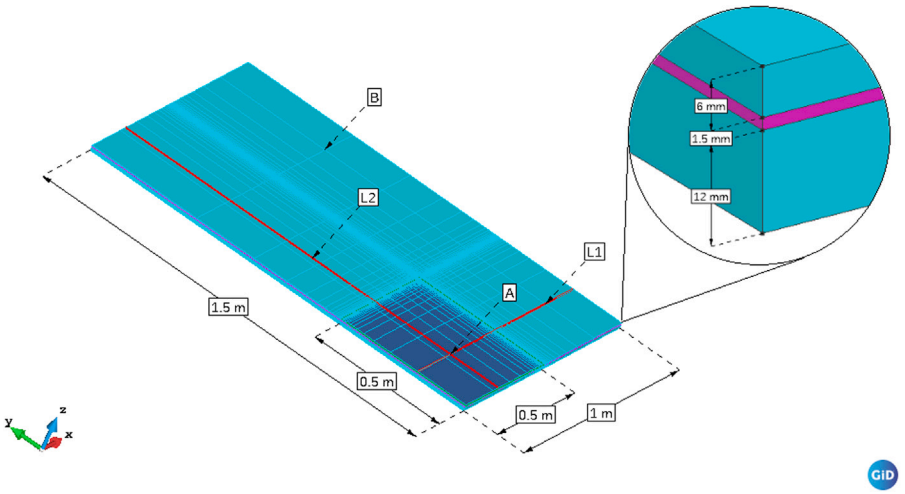

Fig. 4. Example 3. Laminated glass pane with unshaded and shaded portions: geometry and mesh used in the FEM implementation, plotted with the GiD pre-processor.

and inclination (Demain, Journée, & Bertrand, 2013; Revfeim, 1982). A very used approach (Wright, 1998) consists in assuming that the heat flux varies linearly in the thickness of each layer (Galuppi & Royer-Carfagni, 2023a). In our notation, this represents a heat source $q^\sharp(z,t)$ of uniform magnitude in each layer, independent on x, y. This also justifies the use of linear shape functions for approximating $H_z^\sharp(\mathbf{x},t)$, while setting $H_x^\sharp(\mathbf{x},t) = H_y^\sharp(\mathbf{x},t) = 0$. We can assume, following Galuppi and Royer-Carfagni (2022), that part of the energy hitting the external ply at $z = 0$ is absorbed, another part is reflected and the remain part is transmitted to second layer. Similarly, the energy hitting layer 2 splits into an absorbed part, a reflected part, and a part transmitted to layer 3. Denoting with α_i and τ_i the absorptivity and the transmissivity with respect to the solar radiation of the ith ply, the heat it absorbs is

$$q_i^\sharp(\mathbf{x}) = \dot{H}_{z;i}^{\sharp\,\prime}(\mathbf{x}) = \frac{\alpha_i\ \beta_i}{s_i}\ G\,, \qquad \text{where } \beta_i := \begin{cases} 1 & \text{for } i = 1\,, \\ \prod_{k=1}^{i-1} \tau_k & \text{for } i = 2,3\,. \end{cases} \tag{4.3}$$

This allows to define the heat displacement field $\dot{H}_z^\sharp(\mathbf{x})$ through its nodal values. Here, it has been set to be zero at the external surface $z = 0$, while $\tilde{H}_z^\sharp(x,y,s_1) = \alpha_1\beta_1 \int_0^t G dt$, $\tilde{H}_z^\sharp(x,y,s_1+s_2) = (\alpha_1\beta_1 + \alpha_2\beta_2)\int_0^t G dt$, $\tilde{H}_z^\sharp(x,y,s) = (\alpha_1\beta_1 + \alpha_2\beta_2 + \alpha_3\beta_3)\int_0^t G dt$. An arbitrary additive constant could be added to this field (for example, so to have $\tilde{H}_z^\sharp(z,t) = 0$ at the internal surface $z = s$), without affecting the final results.

Realistic values for a winter scenario have been considered for the environmental parameters: $G = 800$ W/m^2, θ_e = -12 °C and θ_i =25 °C. The total external and internal heat transfer coefficients, respectively $h_e = 11.926$ W/(m^{2}K) and $h_i = 8.375$ W/(m^{2}K), have been calculated following Galuppi and Royer-Carfagni (2022). The initial temperature is assumed to be $\theta_0 = 0$ °C.

The heat displacement field has been evaluated by solving the matrix problem (3.7), accounting for the Robin boundary conditions at the two panel surfaces. The panel edges have been assumed to be perfectly insulated, i.e., the normal heat flux is zero on the panel borders. Once the heat displacement field is known, the temperature distribution has been recovered by integrating the internal constrain (2.1) (Fourier's law), calculating the integration constants from the boundary conditions.

Fig. 5 shows the qualitative temperature distribution at the steady state, at the external ($z = s$) and internal ($z = 0$) surfaces. It is evident that they are both approximately uniform in the shaded and not-shaded regions, left aside a thin strip in correspondence of the interface. A comparable example with a partially shaded rectangular portion, but in which the pane is monolithic, was considered in Galuppi and Royer-Carfagni (2023b), implementing the classical version of Biot's variational principle and a different FE implementation. In that simulation, the temperature field presented singularities at the corner, which were attributed to the irregularity (sharp angle) of the interface boundary (Fox, 1971; Yosibash, 2012). Now, it has been verified that the solution presents a very slight peak in the temperature field at the corner of the shaded region, but apparently does not grow unboundedly. Remarkably, the temperature peak disappears if the angle formed by the interface lines at the corners is just slightly different from 90°: the plots in Fig. 5 have been obtained for an 89.5° angle. However, the discussion about the potential concentration of temperatures in areas of high curvature is beyond the scope of this article.

The obtained results are compared with a direct numerical solution of the differential form of the heat-conduction equations, under the aforementioned boundary and initial conditions. This is done with the "pdepe" Matlab tool (MATLAB, 2023), based on a finite difference approach in both space and time. In this case, the plate has been discretized by using tetrahedral elements, with max size of 15 mm and minimum size of 1 mm, for a total of 129 328 elements and 219 004 nodes.

Fig. 6 shows the time variation of the temperatures at the internal ($z = 0$) and external ($z = s$) surfaces, as well as of the interface temperatures at $z = s_1$ and $z = s_2$, at two different (x, y) coordinates of the laminated panel. Fig. 6(a) considers a point A of the shaded region far from the interface (where the temperature is constant in practice at the steady state), whereas Fig. 6(b) refers to

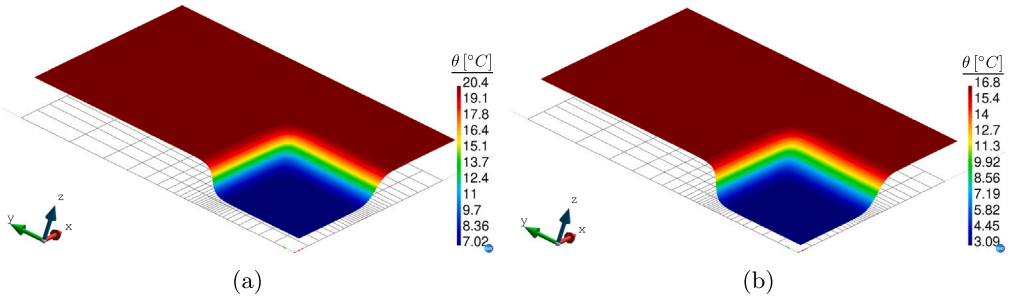

Fig. 5. Example 3. Temperature distribution at the steady state, at (a) the internal $z = 0$ and (b) the external $z = s$ surfaces, plotted with the GiD post-processor.

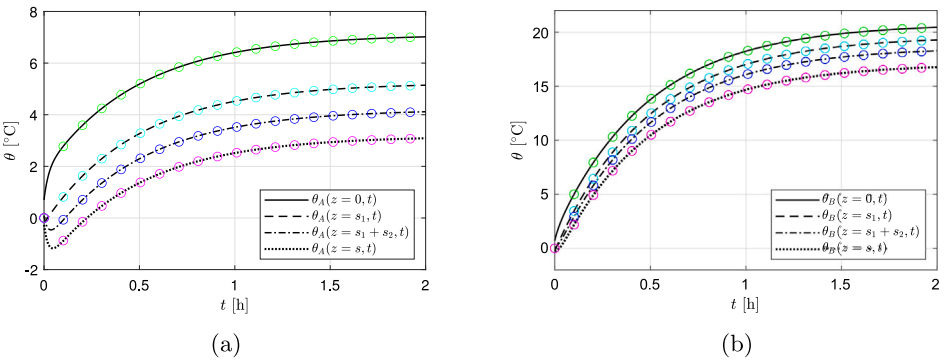

Fig. 6. Example 3. Temperature as a function of time t on the external ($z = s$) and internal ($z = 0$) surfaces and at the interfaces ($z = s_1$ and $z = s_2$), in the (a) irradiated and (b) shaded regions. Comparisons between the proposed approach (lines) and the numerical solution of the differential form of the heat-conduction equations (markers).

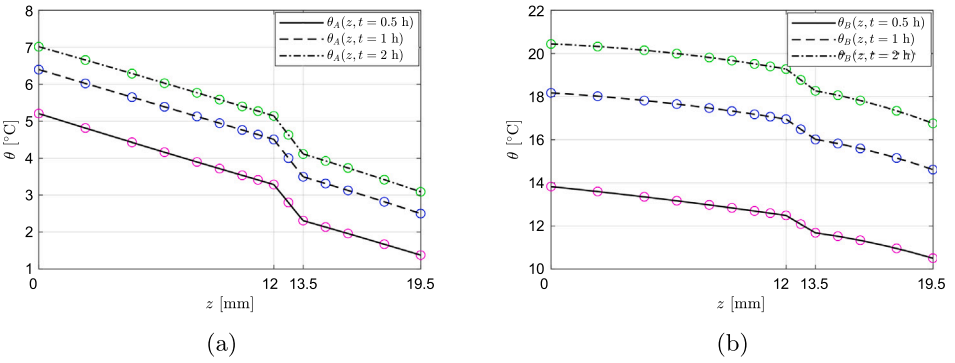

Fig. 7. Example 3. Through-the-thickness temperature profile at different times at the same points considered in Fig. 6. Comparisons between the proposed solutions (lines) and the numerical solution of the differential form of the heat-conduction equations (markers).

a point B of the fully irradiated region, again far from the interface, both indicated in Fig. 4. The graphs also show the comparison with the direct numerical solution, plotted with markers. The steady state condition is achieved in about two hours.

For the same points A and B, Fig. 7 records the temperature profile across the thickness of the laminated glass element, for different time instants.

To analyze the in-plane temperature distribution, Fig. 8 shows the surface and interface temperatures, at the steady state ($t = 2$ h), on the lines L_1 and L_2 indicated in Fig. 4. These graphs emphasize the sigmoidal temperature profile in proximity of the interfaces. The transition zone has a width of about ten times the thickness of the whole laminated panel, which confirms the findings of Galuppi and Royer-Carfagni (2023b).

The comparison with the solution obtained from the differential form of the thermal problem indicates an excellent agreement with our method, being the maximum difference less than 0.2 °C. It has also been verified, in a simpler model problem, that the pde solution requires a much higher number of elements than the proposed approach to obtain comparable results. Since

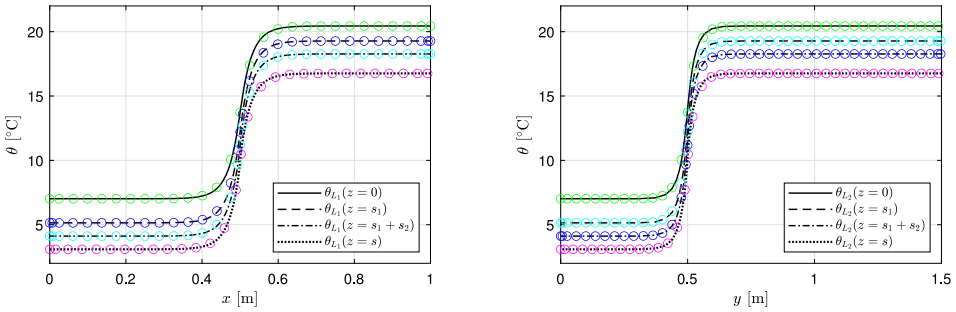

Fig. 8. Example 3. In-plane temperature distribution at the steady state, on the external and internal surfaces and at the interfaces, calculated on the lines (a) L_1 and (b) L_2 of Fig. 4. Comparisons between the proposed approach (lines) and the numerical solution of the differential form of the heat-conduction equations (markers).

the computational time is comparable for the two methods kept fixed the number of nodes, we deduce that our approach is computationally much more efficient.

5. Conclusions

We have presented a variational setting for the heat conduction problem in solid bodies which develops Biot's original formulation, providing the weak form of the energy conservation while Fourier's equation is a holonomic constraint embedded in the formulation. This represents a development of Biot's approach, since only the heat displacement field enters in the equations, whereas Fourier's law is only used *a posteriori* to recover the temperature field. For the one-dimensional case, there is a direct mechanical analogy with the equilibrium problem of an elastic bar with viscous constraints.

The proposed variational formulation has been implemented in a FE framework and applied to benchmark problems, showing an excellent agreement with results taken from the technical literature. Compared to the standard formulations for heat conduction in solids based on the scalar temperature field, one main advantage in the proposed vector field (flux-based) approach is that the heat displacement enjoys a much higher regularity than the temperature. Therefore, its use is particularly convenient in all those problems involving significant temperature gradients, since a coarser discretization is sufficient. With respect to Biot's classical principle, the proposed form allows to use elementary tri-linear shape functions for the displacement field. Numerical convergence is fast and the results accurate.

There are certainly important issues, yet to be investigated. The heat displacement cannot be uniquely determined, yet the heat displacement functions are the primary unknowns of the formulation. The numerical approach has been tested for a limited number of problems, but it is critically important to study the stability character of the proposed formulation. This shall include the study of the Ladyzhenskaya–Babuška–Brezzi (LBB) or inf–sup conditions, performing patch tests and conducting convergence analysis on a higher number of numerical experiments. The weak form of the thermal equations could also be extended to problems characterized by nonlinear heat conduction laws. The formal correspondence between the heat displacement field in the thermal problem, and the displacement field in an elastic problem, detailed in the mechanical analogy for the one-dimensional case, suggests that there may be a commonality of numerical formulation for the coupled thermoelastic problem, yet to be appreciated.

While these issues shall be addressed in further research, the results obtained so far show that the proposed flux-based variational approach is very promising for transient thermal analysis in many applications of structural engineering. We close with a quote from the classic treatise "The Analytical Theory of Heat" published by Joseph Fourier in 1822: *The effects of heat are subject to constant laws which cannot be discovered without the aid of mathematical analysis*.

CRediT authorship contribution statement

Ali Haydar: Writing – original draft, Validation, Software, Methodology, Conceptualization. **Laura Galuppi:** Writing – original draft, Validation, Investigation, Formal analysis. **Gianni Royer-Carfagni:** Writing – review & editing, Supervision, Methodology, Investigation, Formal analysis, Validation, Conceptualization.

Declaration of competing interest

The authors declare that they have no known competing financial interests or personal relationships that could have appeared to influence the work reported in this paper.

Data availability

No data was used for the research described in the article.

Acknowledgments

This research did not receive any specific grant from funding agencies in the public, commercial, or not-for-profit sectors. AH gratefully acknowledges the partial support of his Ph.D. scholarship at the University of Parma by Maffeis Engineering, Sologna (Vi), Italy.

References

Alvarez, G., Flores, J. J., & Estrada, C. A. (1998). The thermal response of laminated glass with solar control coating. *Journal of Physics D (Applied Physics)*, *31*(21), 3057.

Bathe, K.-J. (2006). *Finite element procedures*. Watertown, MA: Klaus-Jurgen Bathe.

Benveniste, Y., & Miloh, T. (1986). The effective conductivity of composites with imperfect thermal contact at constituent interfaces. *International Journal of Engineering Science*, *24*(9), 1537–1552.

Bersani, A. M., & Caressa, P. (2021). Lagrangian descriptions of dissipative systems: a review. *Mathematics and Mechanics of Solids*, *26*(6), 785–803.

Biot, M. A. (1955). Variational principles in irreversible thermodynamics with application to viscoelasticity. *Physical Review*, *97*, 1463–1469.

Biot, M. A. (1957). New methods in heat flow analysis with application to flight structures. *Journal of the Aeronautical Sciences*, *24*(12), 857–873.

Biot, M. A. (1967). Complementary forms of the variational principle for heat conduction and convection. *Journal of the Franklin Institute*, *283*(5), 372–378.

Biot, M. A. (1970). *Variational principles in heat transfer. A unified Lagrangian analysis of dissipative phenomena*. London: Oxford University Press.

Carrot, C, Bendaoud, A, Pillon, C, Olabisi, O, & Adewale, K (2016). Polyvinyl butyral. In *Handbook of thermoplastics, red.* (pp. 89–138). ACRC Press.

Carslaw, H. S., & Jaeger, J. C. (1947). *Conduction of heat in solids*. Oxford: Clarendon Press.

Carter, J. P., & Booker, J. R. (1989). Finite element analysis of coupled thermoelasticity. *Computers and Structures*, *31*(1), 73–80.

Chambers, L. L. G. (1956). A variational principle for the conduction of heat. *The Quaterly Journal of Mechanics and Applied Mathematics*, *9*(2), 234–235.

Chen, J., Xu, X., Zhou, J., & Li, B. (2022). Interfacial thermal resistance: Past, present, and future. *Reviews of Modern Physics*, *94*(2), Article 025002.

Coll, A., Ribó, R., Pasenau, M., Escolano, E., Perez, J Suit, Melendo, A, Monros, A, & Gárate, J (2018). GiD v.14 user manual.

Demain, C., Journée, M., & Bertrand, C. (2013). Evaluation of different models to estimate the global solar radiation on inclined surfaces. *Renewable Energy*, *50*, 710–721.

(2007). *EN ISO 6946 – Building components and building elements – Thermal resistance and thermal transmittance – Calculation method*: *Standard*, ISO/TC 163 and CEN/TC 89.

(2012). *EN 572-1 – Glass in building – Basic soda lime silicate glass products. Part 1: Definitions and general physical and mechanical properties*: *Standard*, CEN/TC 129.

Fox, L. (1971). Some experiments with singularities in linear elliptic partial differential equations. *Proceedings of the Royal Society of London. Series A*, *323*(1553), 179–190.

Furmański, P. (1997). Heat conduction in composites: Homogenization and macroscopic behavior. *Applied Mechanics Reviews*, *50*(6), 327–356.

Galuppi, L., Franco, A., & Bedon, C. (2023). Architectural glass under climatic actions and fire: Review of state of the art, open problems and future perspectives. *Buildings*, *13*(4), 939.

Galuppi, L., & Royer-Carfagni, G. (2022). Biot's Variational Method to determine the thermal strain in layered glazings. *International Journal of Solids and Structures*, *249*, Article 111657.

Galuppi, L., & Royer-Carfagni, G. (2023a). Thermal analysis of architectural glazing in uneven conditions based on Biot's variational principle: Part I - Description of the finite element modelling. *Glass Structures and Engineering*, 1–16.

Galuppi, L., & Royer-Carfagni, G. (2023b). Thermal analysis of architectural glazing in uneven conditions based on Biot's variational principle: Part II - Validation and case-studies. *Glass Structures and Engineering*, 1–24.

Groh, R. M. J., & Weaver, Paul M. (2016). Deleterious localized stress fields: the effects of boundaries and stiffness tailoring in anisotropic laminated plates. *Proceedings of the Royal Society of London. Series A*, *472*(2194), Article 20160391.

Ismail, K. A. R., & Henríquez, J. R. (2003). Modeling and simulation of a simple glass window. *Solar Energy Materials and Solar Cells*, *80*(3), 355–374.

(2003). *ISO 15099 – Thermal performance of windows, doors and shading devices – Detailed calculation*: *Standard*, ISO/TC 163/SC 2.

Lardner, T. J. (1963). Biot's variational principle in heat conduction. *AIAA Journal*, *1*(1), 196–206.

Liang, Zhi, & Hu, Ming (2018). Tutorial: Determination of thermal boundary resistance by molecular dynamics simulations. *Journal of Applied Physics*, *123*(19).

Lienhard, J. H. V, & Lienhard, J. H. IV (2019). *A heat transfer textbook* (5th ed.). Phlogiston Press.

Lipton, R., & Vernescu, B. (1996). Composites with imperfect interface. *Proceedings of the Royal Society of London. Series A*, *452*(1945), 329–358.

Lorenzini, E. (1970). A variational formulation applied to heat conduction equation. *Bulletin de la Classe des Sciences, Academie Royale de Belgique*, *56*(1), 367–379.

Marino, C., Nucara, A., Pietrafesa, M., & Polimeni, E. (2017). The effect of the short wave radiation and its reflected components on the mean radiant temperature: modelling and preliminary experimental results. *Journal of Building Engineering*, *9*, 42–51.

MATLAB (2023). *version R2023a - academic use*. Natick, Massachusetts: The MathWorks Inc..

Mills, Anthony F. (1992). *Heat transfer*. CRC Press.

Mittelstedt, C., Becker, W., Kappel, A., & Kharghani, N. (2022). Free-edge effects in composite laminates - A review of recent developments 2005–2020. *Applied Mechanics Reviews*, *74*(1), Article 010801.

(2004). *N180E – Glass and thermal safety*: *Standard*, CEN/TC129/WG8 – Pilkington.

Nan, C.-W., Birringer, R., Clarke, D. R., & Gleiter, H. (1997). Effective thermal conductivity of particulate composites with interfacial thermal resistance. *Journal of Applied Physics*, *81*(10), 6692–6699.

Nguyen, Q. S. (1994). Bifurcation and stability in dissipative media (plasticity, friction, fracture). *Applied Mechanics Reviews*, *47*(1), 1–31.

Noda, N. (1991). Thermal stresses in materials with temperature-dependent properties. *Applied Mechanics Reviews*, *44*(9), 383–397.

Pásztory, Z., & Le Duong, H. A. (2021). An overview of factors influencing thermal conductivity of building insulation materials. *Journal of Building Engineering*, *44*, Article 102604.

Pietrak, Karol, & Wisniewski, Tomasz S. (2014). Methods for experimental determination of solid-solid interfacial thermal resistance with application to composite materials. *Journal of Power Technologies*, *94*(4), 270.

Revfeim, K. J. A. (1982). Simplified relationships for estimating solar radiation incident on any flat surface. *Solar Energy*, *28*(6), 509–517.

Rosen, P. (1953). On variational principles for irreversible processes. *Journal of Chemical Physics*, *21*(7), 1220–1221.

Ruan, K., Shi, X., Guo, Y., & Gu, J. (2020). Interfacial thermal resistance in thermally conductive polymer composites: a review. *Composites Communications*, *22*, Article 100518.

Sadineni, S. B., Madala, S., & Boehm, R. F. (2011). Passive building energy savings: A review of building envelope components. *Renewable and Sustainable Energy Reviews*, *15*(8), 3617–3631.

Strobel, C. S., Abadie, M. O., & Mendes, N. (2007). Absorption of solar radiation in thick and multilayered glazing. In *Building simulation 2007 conference, Beijing, China*.

Virga, E. G. (2015). Rayleigh-Lagrange formalism for classical dissipative systems. *Physical Review E*, *91*(1), Article 013203.
Wang, L., Guo, J., & Wang, J. (2023). A continuum mixture model for transient heat conduction in multi-phase composites. *International Journal of Engineering Science*, *193*, Article 103934.
Wang, B., Li, J. E., & Yang, C. (2015). Thermal shock fracture mechanics analysis of a semi-infinite medium based on the dual-phase-lag heat conduction model. *Proceedings of the Royal Society of London. Series A*, *471*(2174), Article 20140595.
Wright, J. L. (1998). Calculating center-glass performance indices of windows. *ASHRAE Transactions*, *121*.
Yosibash, Z. (2012). *Singularities in elliptic boundary value problems and elasticity and their connection with failure initiation*. Springer.
Yuan, W., Yu, N., Li, L., & Fang, Y. (2022). Heat transfer analysis in multi-layered materials with interfacial thermal resistance. *Composite Structures*, *293*, Article 115728.
Zienkiewicz, O. C., Taylor, R. L., & Zhu, J. Z. (2005). *The finite element method: its basis and fundamentals*. Elsevier.